

Article

Role of Ag^+ in the Bioleaching of Arsenopyrite by *Acidithiobacillus ferrooxidans*

Yan Zhang ¹, Qian Li ¹ and Xiaoliang Liu ^{2,*} 

¹ School of Minerals Processing and Bioengineering, Central South University, Changsha 410083, China; yanzhang27@csu.edu.cn (Y.Z.); csuliqian208018@csu.edu.cn (Q.L.)

² College of Chemical and Environmental Engineering, Shandong University of Science and Technology, Qingdao 266590, China

* Correspondence: xiaoliang.liu@csu.edu.cn; Tel.: +86-151-1112-6057

Received: 13 February 2020; Accepted: 19 March 2020; Published: 22 March 2020



Abstract: Arsenopyrite (FeAsS) is often associated with gold, but pre-treatment is necessary prior to gold leaching, mainly due to the gold encapsulation in the matrix of FeAsS . Bio-oxidation is attractive and promising, largely due to its simplicity, low cost and environmental friendliness. A critical problem that still impedes the large-scale applications of this green technology is its slow leaching kinetics. Some metal ions such as Ag^+ have previously been found to expedite the bioleaching process. In this paper, the role of Ag^+ in the arsenopyrite bioleaching by *Acidithiobacillus ferrooxidans* was investigated in detail by bioleaching experiments and a series of analyses including thermodynamics, X-ray diffraction (XRD), scanning electron microscopy (SEM) and X-ray photoelectron spectroscopy (XPS). Experimental results suggested that addition of 5 mg/L Ag^+ to the leaching system could significantly improve the final As leaching efficiency from 30.4% to 47.8% and shorten the bioleaching period from 19 days to 15 days. Thermodynamic analysis indicates that Ag^+ destabilises As_2S_2 , As_2S_3 and S^0 via forming Ag_2S , which is confirmed by the XRD analysis on the phase transformation during bioleaching. SEM and XPS analyses further showed that Ag^+ removed the passivating film consisting mainly of As_2S_2 , As_2S_3 and S^0 because Ag_2S formed on the arsenopyrite surface from the start bioleaching of 36 h. In the presence of Fe^{3+} , Ag_2S could easily be dissolved to Ag^+ again, likely leading to the establishment of the $\text{Ag}^+/\text{Ag}_2\text{S}$ cycle. The bacteria utilised the two synergistic cycles of $\text{Fe}^{3+}/\text{Fe}^{2+}$ and $\text{Ag}^+/\text{Ag}_2\text{S}$ to catalyse the bioleaching of arsenopyrite.

Keywords: arsenopyrite; gold ore; bioleaching; passivating film; metal ion catalyst; silver

1. Introduction

In nature, significant amounts of gold are often found in arsenopyrite (FeAsS) [1–3]. However, most gold in the arsenopyrite is difficult to leach, mainly because the gold tends to be encapsulated in the mineral matrix [4,5]. It is, thus, necessary to pre-treat arsenopyrite gold ores before leaching to improve gold extraction. Currently, four pre-treatment methods are commonly used, i.e., oxidative roasting, chemical oxidation, pressure oxidation and biological oxidation [6,7]. Amongst them, bio-oxidation is a simple, low-cost and eco-friendly technology that is appropriate to extract valuable metals from a series of ores/concentrates and waste materials with substantially reduced environmental pollution. In the past decade, this promising green technology has drawn significant attention, and its applications in bio-hydrometallurgy have also been on the increase [8–10].

Although, many advantages can be provided from bio-oxidation, the problem of slow leaching kinetics still impedes its large-scale application [8,11]. A range of metal ions, including Cu^{2+} , Bi^{3+} , Co^{2+} , Hg^{2+} and Ag^+ have, therefore, been used as catalysts to enhance the dissolution kinetics and shorten the bioleaching period [12,13]. Much attention has been paid to Ag^+ among these metal ions. Significant

researches had suggested that Ag^+ is an efficient catalyst in improving the leaching yields and kinetics of valuable metals from a wide range of copper sulphide minerals, such as chalcopyrite [14–17]. Ag^+ was also shown to effectively enhance the bioleaching of arsenic sulphide minerals, such as realgar and orpiment [18,19].

However, few research effects have been made to investigate the effects of Ag^+ on the bioleaching of arsenopyrite. Research has reported that as $2 \text{ mg}\cdot\text{L}^{-1}$ Ag^+ is added to leaching solution, the bioleaching efficiency of As, from arsenopyrite, could be improved by ~23% for the same leaching duration [20]. Maybe the catalytic effect of Ag^+ is attributed to an autocatalytic role of Ag^+ or formation of an autocatalytic surface. The reason why Ag^+ enhanced the bioleaching of arsenopyrite, and how Ag^+ played its role in the process, remain unclear.

In our recent research [13,21,22], a compact passivating film was found to form on the surface of arsenopyrite from the beginning stage of bioleaching (<36 h), and this film would severely hinder the subsequent leaching process. The formation of this passivating film that was shown to consist mainly of As_2S_2 , As_2S_3 and S^0 was considered as the main reason for the slow leaching kinetics and long leaching periods. Based on these research findings, this paper reports results from a detailed investigation into the role of Ag^+ in the bioleaching of pure arsenopyrite in 9K culture medium containing *Acidithiobacillus ferrooxidans* (*A. ferrooxidans*). This investigation starts with a series of bioleaching experiments on natural samples of pure arsenopyrite. The leachate and leached solid samples were respectively analysed with inductively coupled plasma-atomic emission spectrometry (ICP-AES) for the As and Fe concentrations and with X-ray diffraction (XRD), scanning electron microscopy (SEM) and X-ray photoelectron spectroscopy (XPS) for mineralogical phase, morphology and surface composition. In addition, thermodynamic analyses were conducted to elucidate the reasons for the improved bioleaching kinetics by Ag^+ . The possible mechanisms by which the Ag^+ enhanced the bioleaching of arsenopyrite were also proposed in this paper.

2. Thermodynamic Calculations

The software, HSC Chemistry 6.0 [23], was used to construct the Eh–pH diagrams for the $\text{FeAsS-H}_2\text{O}$ and $\text{FeAsS-Ag}^+-\text{H}_2\text{O}$ systems. The temperature and pressure were set at 25 °C and 1 atm, respectively. Under the leaching conditions of $[\text{Fe}^{2+}]$ 0.16 M, $[\text{FeAsS}]$ 0.06 M (10 g/L) and $[\text{Ag}^+]$ 0.046 mM (5 mg/L; when Ag^+ was present in the leaching system), the predominance areas for Fe, As and S as well as Ag species on relevant Eh (versus the standard hydrogen electrode (SHE)) and pH scales were presented in Eh–pH diagrams. The available thermodynamic data used in the calculations are listed in Appendix A Table A1.

3. Experimental

3.1. Minerals, Strain and Media

The high-purity arsenopyrite sample investigated had a composition of $\text{Fe}_{1.00}\text{As}_{0.99}\text{S}_{0.97}$ and only contained impurities of Si 0.132%, Ni 0.062% and Co 0.034% assayed by X-ray fluorescence analysis. Either particles or cuboids of the arsenopyrite samples were used in this study. The arsenopyrite particles (over 90%, ~74 μm) were obtained by wet-milling in a ball mill whilst the cuboids (~15 mm \times ~15 mm \times ~5 mm) were prepared using a cutter. Air-tight plastic bags were used to store the samples to minimise oxidation.

The bacteria of *A. ferrooxidans* and 9K culture medium containing $\text{FeSO}_4\cdot 7\text{H}_2\text{O}$ 44.8 g/L, $(\text{NH}_4)_2\text{SO}_4$ 3.0 g/L, $\text{K}_2\text{HPO}_4\cdot 3\text{H}_2\text{O}$ 0.50 g/L, KNO_3 0.14 g/L, $\text{Ca}(\text{NO}_3)_2\cdot 4\text{H}_2\text{O}$ 0.01 g/L and $\text{MgSO}_4\cdot 7\text{H}_2\text{O}$ 0.5 g/L were utilised for the bioleaching of arsenopyrite. A total of 100 mL 9K culture medium and 15 mL inoculum were first added to 250 mL Erlenmeyer flasks and then shaken in an orbital thermostat shaker under 160 rpm and 30 °C to culture and sub-culture *A. ferrooxidans*. The medium was adjusted by careful addition of ~3 M H_2SO_4 to have an initial pH value of 1.8. In the presence of 10 g/L arsenopyrite particles, the bacteria had been sub-cultured for three months before the bioleaching experiments.

Silver nitrate (AgNO_3) was utilised as the silver cation (Ag^+) source. The reagents used in the bioleaching experiments of arsenopyrite and the cultivation of bacteria were all analytically pure. De-ionised water was utilised throughout all experiments.

3.2. Bioleaching Experiment

Using the same experimental method and conditions for the cultivation of bacteria, the growth of *A. ferrooxidans* and the bioleaching of arsenopyrite by *A. ferrooxidans* proceeded simultaneously. The addition of Ag^+ to the leaching solution ranged from 1 to 20 mg/L. For the bioleaching of arsenopyrite particles, the pulp density was 10 g/L of FeAsS. Samples from the supernatant were withdrawn at regular intervals during the bioleaching process for chemical analysis. During the bioleaching process, the solution potential and pH values were also measured and recorded. All solution potentials were reported relative to the SHE. The pulp was filtered, washed with copious de-ionised water at least ten times, and dried in a vacuum oven at 35 °C overnight, to attain the residue for the subsequent mineralogical phase study. The morphology and surface composition analyses were conducted on the arsenopyrite cuboids. Prior to each bioleaching experiment, silicon carbide papers of 800, 1500 and 3000 grit were used sequentially to polish the cuboids, and then the contaminants on the surface of cuboids were cleaned ultrasonically in alternate baths of 5 M HCl, methanol and water for 5 min [24,25].

3.3. Analytical Methods

The concentrations of As and Fe in leachate were determined by ICP-AES (PS-6, Baird). Potassium dichromate titration method was used to determine the concentration of Fe^{2+} . The difference between the concentration of the total Fe and Fe^{2+} obtained the Fe^{3+} concentration. A pH meter (PHSJ-4A, Shanghai Leici, Shanghai, China) equipped with a Pt electrode and Ag/AgCl (saturated KCl, Orion) reference electrode was used to measure the values of solution potential and pH. An X-ray diffractometer (D/Max 2500, Rigaku, Hiroshima, Tokyo, Japan) was used to determine the mineralogical phases of the bioleached residue. An SEM (Helios NanoLab G3 UC, FEI, Hillsboro, OR, USA) was used to examine the morphology of leached cuboids. The Ag species on the surface of the leached cuboid was analysed with XPS (ESCALAB250Xi, Thermo Fisher, Waltham, MA, USA).

4. Results and Discussion

4.1. Effect of Ag^+ Addition on Arsenopyrite Bioleaching

The kinetic results from the arsenopyrite bioleaching are shown in Figure 1. As the leaching behaviour of As from arsenopyrite acts as a critical indicator for the bioleaching of arsenopyrite [13,21,22], the effect of Ag^+ on arsenopyrite bioleaching can be evaluated by its influence on the change of As leaching efficiency during bioleaching, as shown in Figure 1a. In contrast with the slow bioleaching kinetics of As without Ag^+ , the addition of Ag^+ to the solution was shown to substantially enhance the bioleaching of As, and thus, arsenopyrite as manifested by the marked rise in the leaching efficiency of As during bioleaching. The optimal concentration of Ag^+ was shown to be 5 mg/L. Under this Ag^+ level, the final leaching efficiency of As was noticeably increased from 30.4% without Ag^+ to 47.8%. The bioleaching period was also shortened from 19 days to 15 days. The presence of Ag^+ made the bioleaching of As much faster than the situation without Ag^+ from the initial leaching stage. After leaching 1 day, the As leaching efficiency was markedly increased from 2.4% without Ag^+ to 12.3% with 5 mg/L Ag^+ . Obviously, when Ag^+ (5 mg/L) was contained in the solution, the passivation of the arsenopyrite surface that took place initially during bioleaching, as reported in our recent researches [13,21], was greatly weakened and even disappeared. When the concentration of Ag^+ exceeded 5 mg/L, the bioleaching deteriorated as the As leaching efficiency started to decrease. This phenomenon can be explained by the fact that an excess of Ag^+ have detrimentally affected the reproduction and activity of bacteria, and thus, the bioleaching of As.

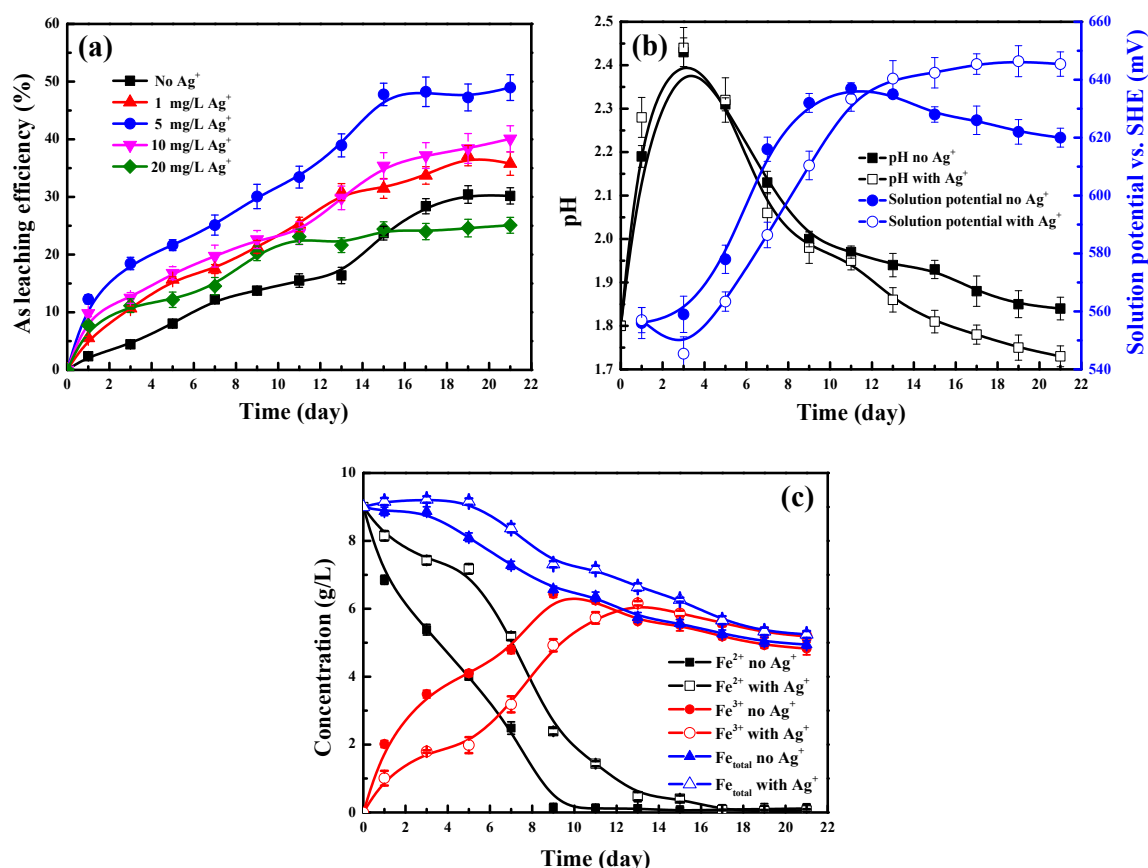


Figure 1. Effect of Ag^+ concentration on the (a) leaching efficiency of As and variation of (b) pH and solution potential and (c) concentrations of Fe^{3+} , Fe^{2+} and total Fe in the presence and absence of 5 mg/L Ag^+ during the bioleaching of arsenopyrite particles.

Under the optimal addition of Ag^+ (5 mg/L), Figure 1b,c show the variation of pH and solution potential, as well as concentrations of iron ions including Fe^{3+} , Fe^{2+} and total Fe during bioleaching. As shown in Figure 1b, a similar variation trend of pH was found regardless if Ag^+ was present in the solution. The pH rose noticeably with the growth of bacteria in the initial leaching of 3 days. At the later stage (>3 days), the pH decreased, mainly due to the oxidative dissolution of arsenopyrite [13,21]. The bioleaching process is closely related to the solution potential, which is largely determined by the $\text{Fe}^{3+}/\text{Fe}^{2+}$ couple in the leaching system. A similar change trend between the solution potential and the Fe^{3+} concentration was clearly seen from Figure 1b,c. A greater solution potential can offer a stronger driving force for the bioleaching of arsenopyrite [13,21]. The presence of Ag^+ (5 mg/L) was found to cause a much lower Fe^{3+} concentration and a higher Fe^{2+} concentration (Figure 1c) and thus a lower level of solution potential (Figure 1b). However, a much higher leaching efficiency of As (Figure 1a) was still achieved, further confirming the catalytic effect of Ag^+ (5 mg/L). As will be demonstrated in the following sections, a series of analyses of thermodynamics, mineralogical phase, morphology and surface composition were conducted to elucidate why, and how, Ag^+ played this catalytic effect.

4.2. Thermodynamics of Arsenopyrite Dissolution in the Presence of Ag^+

The Eh–pH diagrams of $\text{FeAsS}-\text{H}_2\text{O}$ and $\text{FeAsS}-\text{Ag}^+-\text{H}_2\text{O}$ systems are presented in Figure 2a–c and 2a'–d', respectively.

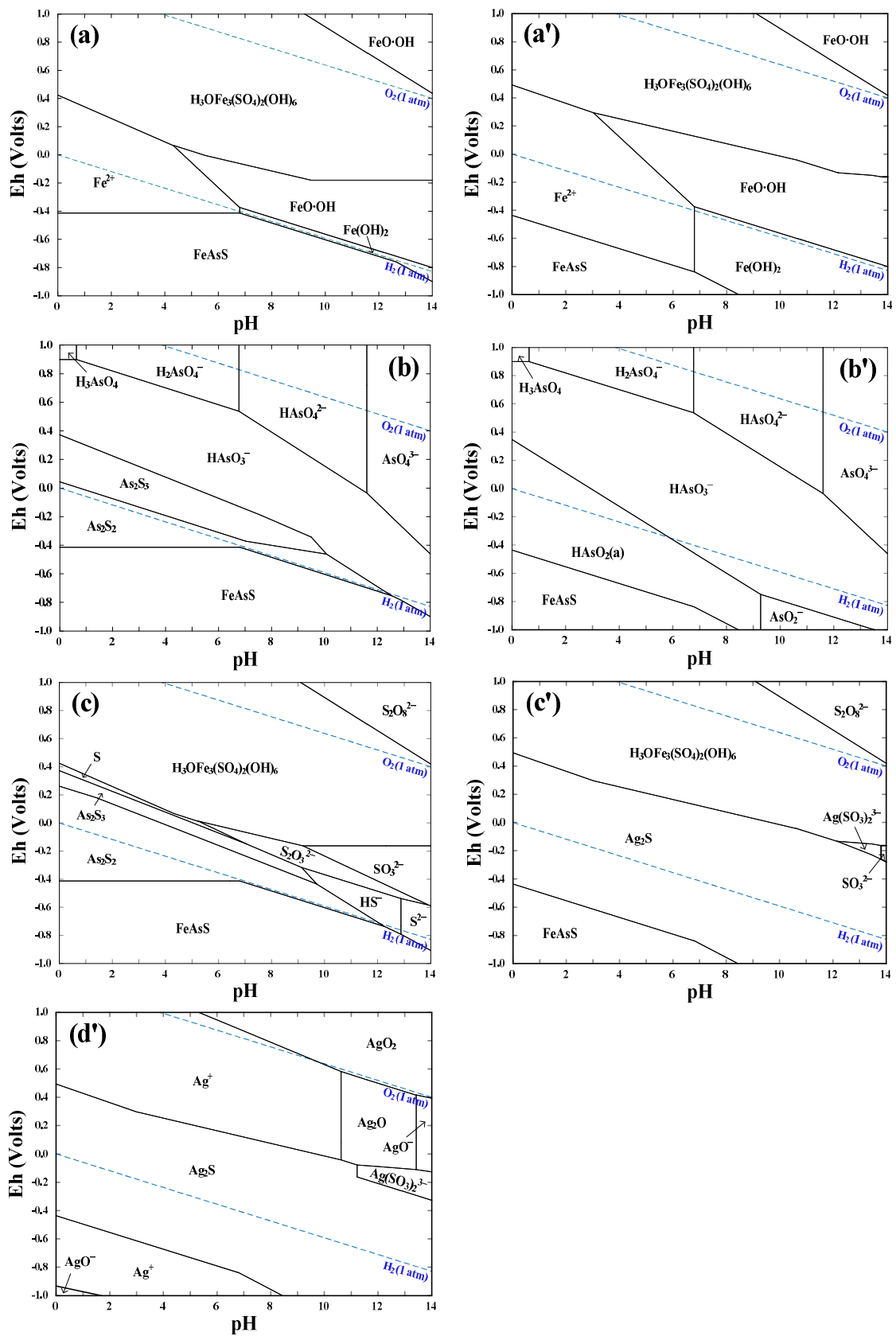


Figure 2. Eh–pH diagrams of (a)–(c) FeAsS–H₂O system and (a')–(d') FeAsS–Ag⁺–H₂O system for (a)/(a') Fe species, (b)/(b') As species, (c)/(c') S species and (d') Ag species. Conditions: [Fe²⁺] 0.16 M, [FeAsS] 0.06 M, [Ag⁺] 0.046 mM; 25 °C and 1 atm.

In the pH range of 0–3 that is a typical acidic bioleaching condition, Figure 2a–c show that, in the absence of Ag^+ , an Eh higher than -0.4 V can drive the oxidative dissolution of arsenopyrite. In the Eh–pH region of -0.4 – 0.4 V and 0–3, the predominant species of Fe, As and S are Fe^{2+} (Figure 2a), $\text{As}_2\text{S}_2/\text{As}_2\text{S}_3$ (Figure 2b), and $\text{As}_2\text{S}_2/\text{As}_2\text{S}_3/\text{S}^0$ (Figure 2c), respectively. As demonstrated previously [13,21], the solid species of As_2S_2 , As_2S_3 and S^0 are the main intermediate products that would form a passivating film on the arsenopyrite surface, causing a severe hindrance to the bioleaching process. Under an Eh higher than 0.2 – 0.4 V, $\text{H}_3\text{OFe}_3(\text{SO}_4)_2(\text{OH})_6$ in Figure 2a,c is shown to be the main phase for the Fe and S species while HAsO_3^- and H_2AsO_4^- in Figure 2b are the main phase for the As species. Note that, in the 9K culture medium, $\text{H}_3\text{OFe}_3(\text{SO}_4)_2(\text{OH})_6$ and K^+ can readily form jarosite [$\text{KFe}_3(\text{SO}_4)_2(\text{OH})_6$] [26,27].

Comparing Figure 2a–c with 2a'–c', the addition of 0.046 mM (5 mg/L) Ag^+ to the FeAsS– H_2O system leads to significant changes in the predominance regions for Fe, As and S species. Figure 2a,a' show that, within pH of 0–3, a much lower Eh (> -0.44 – -0.62 V) is required to leach the Fe from FeAsS as Fe^{2+} to the leaching solution, whilst a much higher Eh (> 0.3 – 0.5 V) is needed for the transformation of Fe^{2+} to $\text{H}_3\text{OFe}_3(\text{SO}_4)_2(\text{OH})_6$. The predominance areas of As and S species, i.e., As_2S_2 , As_2S_3 and S^0 in Figure 2b,c change to those of HAsO_2 (a) and Ag_2S as shown in Figure 2b',c'. In common with the formation of Fe^{2+} , HAsO_2 (a) and Ag_2S can also be formed at a lower Eh (> -0.44 – -0.62 V). Therefore, thermodynamically, the presence of Ag^+ makes As_2S_2 , As_2S_3 and S^0 unstable by forming Ag_2S . In addition, Figure 2d' shows that the predominant Ag species is Ag_2S , which is readily converted to Ag^+ at an Eh higher than 0.3 – 0.5 V. This means that the oxidative dissolution of Ag_2S into the solution can easily take place in the presence of the $\text{Fe}^{3+}/\text{Fe}^{2+}$ couple ($E^\circ = 0.771$ V versus SHE).

4.3. Mineralogical Phase Transformation

To determine the effect of Ag^+ (5 mg/L) on the transformation of mineralogical phase, XRD surveys were performed on bioleached arsenopyrite particles for different days. As the passivation took place from the onset of bioleaching [13,21], the phase change was investigated for the initial leaching stage (< 3 days). The XRD diffractograms are presented in Figure 3.

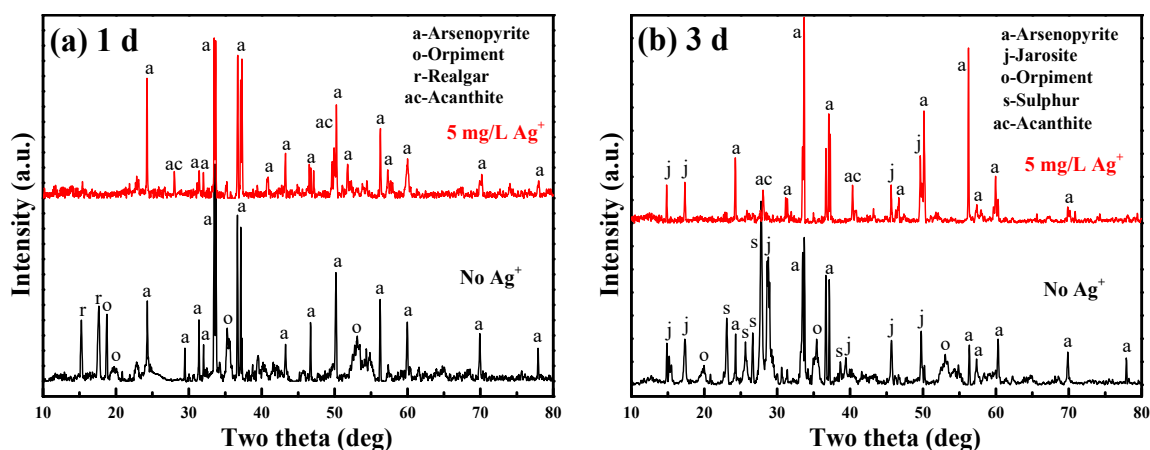


Figure 3. XRD diffractograms of the bioleached arsenopyrite particles after leaching (a) 1 day and (b) 3 days with and without 5 mg/L Ag^+ .

Without the addition of Ag^+ , the phases of realgar (As_2S_2) and orpiment (As_2S_3) occurred after bioleaching 1 day (Figure 3a). Elemental sulphur (S^0) and jarosite [$\text{KFe}_3(\text{SO}_4)_2(\text{OH})_6$] were also found after 3 days (Figure 3b). With the addition of Ag^+ at 5 mg/L, however, Figure 3a,b shows that the passivating phases of As_2S_2 , As_2S_3 and S^0 disappeared with the formation of acanthite (Ag_2S). This agrees well with the thermodynamic predictions in Section 4.2.

4.4. Morphology and Surface Composition Changes

SEM and XPS analyses were further conducted to reveal the effect of Ag^+ (5 mg/L) on the morphology and surface composition of the bioleached arsenopyrite cuboids. During the bioleaching process, considerable amounts of jarosite were observed to form after around 5 days whether Ag^+ was added to the solution or not. However, our recent research suggested that the precipitates of jarosite only formed a loose and porous overlayer, instead of a passivating film, on the surface of arsenopyrite [13,21]. The surface was investigated just for the initial leaching stage (i.e., 36 h) to avoid the interference from jarosite. The SEM images and XPS spectrum are presented in Figures 4 and 5, respectively.

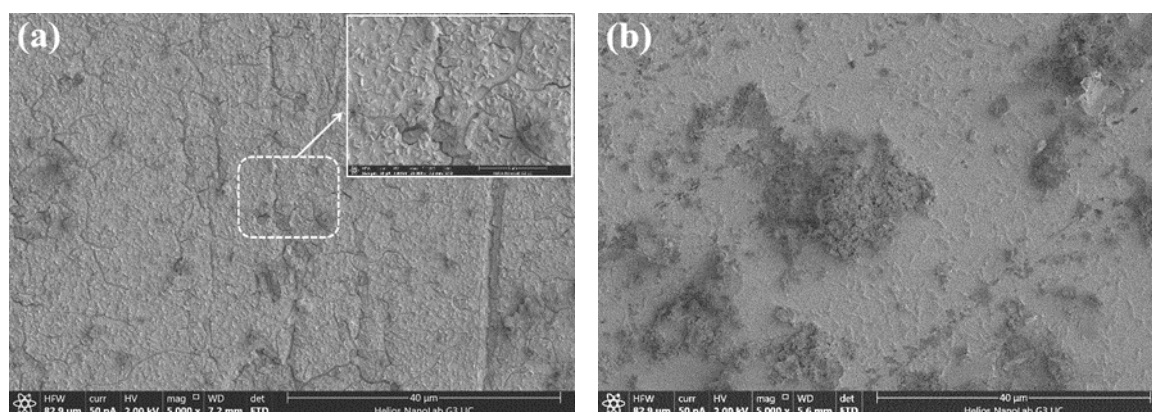


Figure 4. SEM images for the surfaces of arsenopyrite cuboids after bioleaching 36 h in 9K culture medium (a) without and (b) with 5 mg/L Ag^+ .

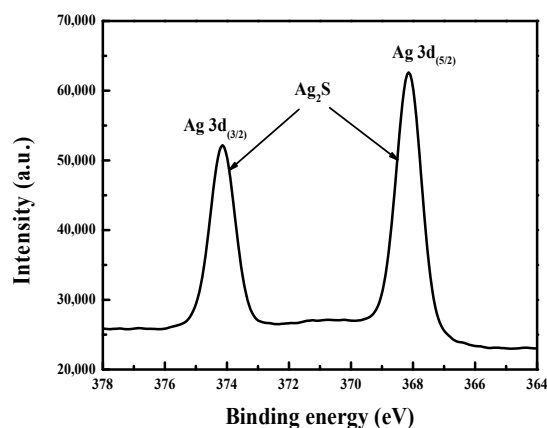


Figure 5. XPS spectrum of Ag 3d for the surface of arsenopyrite cuboid after bioleaching 36 h in 9K culture medium with 5 mg/L Ag^+ .

As clearly seen from Figure 4a, a compact passivating film was formed on the arsenopyrite surface. Note that the film was intact in the solution, and the appearance of the cracks occurred only after drying. The film was shown to consist mainly of As_2S_2 , As_2S_3 and S^0 in our recent researches [13,21]. After bioleaching in the presence of Ag^+ (5 mg/L), no passivating film was observed on the surface, as presented in Figure 4b. As shown in the above XRD analysis, the disappearance of the phases of As_2S_2 , As_2S_3 and S^0 due to the addition of Ag^+ is responsible for the removal of this passivating film.

In addition, Figure 5 shows the XPS spectrum of Ag 3d on the outmost surface of the leached arsenopyrite cuboid at the Ag^+ level of 5 mg/L. Two obvious peaks of $\text{Ag } 3d_{(3/2)}$ and $\text{Ag } 3d_{(5/2)}$ were exhibited. The $\text{Ag } 3d_{(5/2)}$ peak centring at the binding energy of 368.1 eV reflects the typical peak of Ag_2S [28,29].

In summary, the presence of 5 mg/L Ag^+ substantially enhanced the bioleaching efficiency and kinetics (Section 4.1). The XRD, SEM, XPS and thermodynamic results, presented in Sections 4.2–4.4 demonstrated that the inclusion of 5 mg/L Ag^+ in the leaching system could lead to the disappearance of the visible passivating film on the arsenopyrite surface in bioleaching without Ag^+ . The removal of the passivating film that can form at the initial leaching stage (< 36 h) explains why Ag^+ catalyses the whole bioleaching process.

4.5. Possible Mechanisms for the Ag^+ Catalysed Bioleaching of Arsenopyrite

Based on the above experimental and analytical results, the possible mechanism for the silver-catalysed bioleaching of arsenopyrite can be proposed as presented in Figure 6. In addition, the possible reactions involved in the bioleaching process are listed in Table 1.

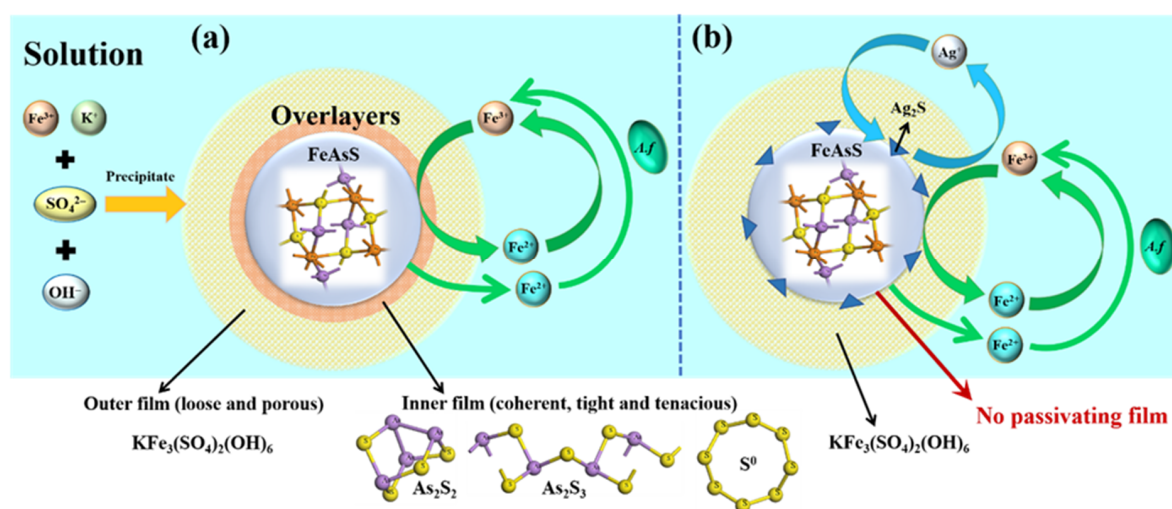


Figure 6. Schematic diagram of the mechanisms for the bioleaching of arsenopyrite (a) without and (b) with Ag^+ .

Table 1. Possible reactions involved in the oxidative leaching of arsenopyrite in the presence of Ag^+ .

Oxidative Dissolution of Arsenopyrite	$\Delta G_r^0/(\text{kJ/mol})^a$	No.
$3\text{FeAsS} + 2\text{H}_2\text{O} + 7\text{Fe}^{3+} = \text{As}_2\text{S}_2 + \text{S}^{2-} + 10\text{Fe}^{2+} + \text{AsO}_2^- + 4\text{H}^+$	-504.203	1
$4\text{FeAsS} + 4\text{H}_2\text{O} + 12\text{Fe}^{3+} = \text{As}_2\text{S}_3 + \text{S}^{2-} + 16\text{Fe}^{2+} + 2\text{AsO}_2^- + 8\text{H}^+$	-816.451	2
$2\text{FeAsS} + 6\text{H}_2\text{O} + 10\text{Fe}^{3+} = \text{S}^0 + 2\text{HAsO}_3^- + \text{S}^{2-} + 12\text{Fe}^{2+} + 10\text{H}^+$	-531.546	3
$3\text{FeAsS} + 2\text{H}_2\text{O} + 2\text{Ag}^+ + 7\text{Fe}^{3+} = \text{Ag}_2\text{S} + \text{As}_2\text{S}_2 + 10\text{Fe}^{2+} + \text{AsO}_2^- + 4\text{H}^+$	-784.910	4
$4\text{FeAsS} + 4\text{H}_2\text{O} + 2\text{Ag}^+ + 12\text{Fe}^{3+} = \text{Ag}_2\text{S} + \text{As}_2\text{S}_3 + 16\text{Fe}^{2+} + 2\text{AsO}_2^- + 8\text{H}^+$	-1097.156	5
$2\text{FeAsS} + 6\text{H}_2\text{O} + 2\text{Ag}^+ + 10\text{Fe}^{3+} = \text{Ag}_2\text{S} + \text{S}^0 + 2\text{HAsO}_3^- + 12\text{Fe}^{2+} + 10\text{H}^+$	-812.255	6
Oxidation of Passivating Products from Arsenopyrite Leaching		
$2\text{As}_2\text{S}_2 + 15\text{H}_2\text{O} + 16\text{Fe}^{3+} = 4\text{HAsO}_3^- + 2\text{S}^{2-} + \text{HS}_2\text{O}_3^- + 16\text{Fe}^{2+} + 25\text{H}^+$	-282.116	7
$\text{As}_2\text{S}_3 + 9\text{H}_2\text{O} + 10\text{Fe}^{3+} = 2\text{HAsO}_3^- + \text{S}^{2-} + \text{HS}_2\text{O}_3^- + 10\text{Fe}^{2+} + 15\text{H}^+$	-177.281	8
$2\text{S}^0 + 3\text{H}_2\text{O} + 2\text{Fe}^{3+} = \text{HS}_2\text{O}_3^- + \text{S}^{2-} + 2\text{Fe}^{2+} + 5\text{H}^+$	-116.431	9
$2\text{As}_2\text{S}_2 + 15\text{H}_2\text{O} + 4\text{Ag}^+ + 16\text{Fe}^{3+} = 2\text{Ag}_2\text{S} + 4\text{HAsO}_3^- + \text{HS}_2\text{O}_3^- + 16\text{Fe}^{2+} + 25\text{H}^+$	-843.533	10
$\text{As}_2\text{S}_3 + 9\text{H}_2\text{O} + 2\text{Ag}^+ + 10\text{Fe}^{3+} = \text{Ag}_2\text{S} + 2\text{HAsO}_3^- + \text{HS}_2\text{O}_3^- + 10\text{Fe}^{2+} + 15\text{H}^+$	-457.990	11
$3\text{S}^0 + 3\text{H}_2\text{O} + 2\text{Ag}^+ + 2\text{Fe}^{3+} = \text{Ag}_2\text{S} + \text{HS}_2\text{O}_3^- + 2\text{Fe}^{2+} + 5\text{H}^+$	-164.276	12
Oxidation of Ag_2S		
$8\text{Fe}^{3+} + 2\text{Ag}_2\text{S} + 3\text{H}_2\text{O} = 8\text{Fe}^{2+} + 4\text{Ag}^+ + \text{HS}_2\text{O}_3^- + 5\text{H}^+$	-26.421	13

^a Values were calculated using the equation of $\Delta G_r^0 = \sum[\nu_i \Delta G_f^0(i)]$, where the values of ΔG_f^0 are listed in Appendix A.

Figure 6a shows that, in the leaching solution without Ag^+ , the bacteria oxidise the Fe^{2+} to Fe^{3+} , which will in turn oxidise the arsenopyrite to achieve its leaching, as shown by Equations (1)–(3) in Table 1. With the bioleaching of arsenopyrite, As_2S_2 , As_2S_3 and S^0 are also produced in situ on the surface of arsenopyrite particles. Although these solid products could be further oxidised according to reactions (7)–(9) listed in Table 1, they still formed a passivating film at the initial bioleaching stage, causing a severe impedance to the subsequent leaching process.

With the addition of Ag^+ to the solution (Figure 6b), the oxidative dissolution of arsenopyrite would proceed according to Equations (4)–(6) with much lower ΔG_r^0 values than those of Equations (1)–(3) (Table 1). In the process, Ag_2S was formed on the surface of arsenopyrite, largely preventing the formation of the passivating products (i.e., As_2S_2 , As_2S_3 and S^0) on the basis of Equations (10)–(12), as evidenced by the results from XRD and XPS analyses. In addition, Ag_2S itself is a conductor that is beneficial for the transfer of electrons in the leaching process. In the presence of Fe^{3+} , Ag_2S can also be oxidised by the $\text{Fe}^{3+}/\text{Fe}^{2+}$ couple according to reaction (13), releasing Ag^+ back to the solution. Therefore, as presented in Figure 6b, a catalytic cycle of $\text{Ag}^+/\text{Ag}_2\text{S}$ was also established from the catalytic cycle of $\text{Fe}^{3+}/\text{Fe}^{2+}$. The two catalytic cycles led to the elimination of the passivating film, as evidenced by the SEM images, i.e., the much improved bioleaching of arsenopyrite.

5. Conclusions

Experimental results from the arsenopyrite bioleaching by *A. ferrooxidans* in 9K culture medium suggested that addition of 5 mg/L Ag^+ to the solution had no significant influence on the pH, but resulted in a lower level of the solution potential. However, the bioleaching of arsenopyrite was still substantially improved from the onset of leaching. On the one hand, the final leaching efficiency of As was significantly increased from 30.4% to 47.8%; on the other hand, the bioleaching period was noticeably shortened from 19 days to 15 days. This is attributed to the fact that the presence of Ag^+ in the solution leads to the removal of the passivating film (being composed mainly of As_2S_2 , As_2S_3 and S^0 [13,21]) that could be formed initially on the surface of arsenopyrite. Thermodynamic and XRD analyses demonstrated that, during the bioleaching of arsenopyrite, Ag^+ could destabilise As_2S_2 , As_2S_3 and S^0 through formation of Ag_2S , which would easily be dissolved to Ag^+ by the $\text{Fe}^{3+}/\text{Fe}^{2+}$ couple. SEM and XPS analyses further suggested that the main difference the Ag^+ caused was that the formation of the passivating film was prevented by Ag^+ via forming Ag_2S on the arsenopyrite surface. On the basis of the combined results from bioleaching experiments, thermodynamic and phase analyses, and surface characterisation, a possible mechanism for the silver catalysed bioleaching of arsenopyrite is put forward that the two synergistic cycles of $\text{Ag}^+/\text{Ag}_2\text{S}$ and $\text{Fe}^{3+}/\text{Fe}^{2+}$ were utilised by the bacteria to improve the leaching of arsenopyrite. The results in this paper can also offer useful information for the extraction of valuable metals from other As- and S-bearing materials.

Author Contributions: Y.Z. and Q.L. conceived and designed the study; Q.L. contributed reagents/materials/analysis tools; Y.Z. performed the experiments; X.L. and Y.Z. analysed the data; X.L. wrote the paper. All authors have read and agreed to the published version of the manuscript.

Funding: This research was funded by the National Natural Science Foundation of China (grant no. 51574284) and the National Key Research and Development Program of China (grant no. 2018YFE0110200).

Acknowledgments: Financial supports from the National Natural Science Foundation of China and the National Key Research and Development Program of China are all gratefully acknowledged.

Conflicts of Interest: The authors declare no conflict of interest.

Appendix A

Table A1. Free energies of formation (kJ/mol) for relevant species ^a.

Species	ΔG_f° / (kJ/mol)	Species	ΔG_f° / (kJ/mol)	Species	ΔG_f° / (kJ/mol)	Species	ΔG_f° / (kJ/mol)
FeAsS	-49.7616	As ₂ S ₂	-68.5508	S	0	AgO	14.50
FeAsO ₄	-772.727	As ₂ S ₃	-91.4907	S ²⁻	86.00982	AgO ₂	-10.996
Fe ₃ (AsO ₄) ₂	-1766.73	As ₂ O ₃	-576.899	S ₂ ²⁻	79.76167	Ag ₂ O	-11.180
Fe(OH) ₂	-492.158	As ₂ O ₄	-701.161	SO ₃ ²⁻	-486.755	Ag ₂ O ₂	27.429
Fe(OH) ₃	-705.885	As ₂ O ₅	-782.437	S ₂ O ₃ ²⁻	-518.87	Ag ₂ O ₃	121.329
FeO·OH	-489.439	As ₄ O ₆	-1152.42	S ₂ O ₄ ²⁻	-600.825	Ag ₂ S	-40.401
Fe ³⁺	-17.1907	AsO ₂ ⁻	-349.991	S ₂ O ₅ ²⁻	-791.217	Ag ₂ SO ₃	-411.615
Fe ²⁺	-91.5644	AsO ₄ ³⁻	-648.477	S ₂ O ₆ ²⁻	-969.453	Ag ²⁺	268.686
FeOH ²⁺	-242.064	As(OH) ₄ ⁻	-824.457	S ₂ O ₇ ²⁻	-795.432	Ag ⁺	77.148
FeOH ⁺	-275.615	HAsO ₃ ⁻	-606.638	S ₂ O ₈ ²⁻	-1115.35	Ag(HS) ₂ ⁻	0.247
Fe(OH) ₂ ⁺	-452.391	HAsO ₄ ²⁻	-714.732	HS ₂ ⁻	11.51053	AgO ⁻	-22.762
Fe ₂ (OH) ₂ ⁴⁺	-467.733	H ₂ AsO ₃ ⁻	-587.149	HSO ₃ ⁻	-527.84	Ag(OH) ₂ ⁻	-260.214
H ₃ OFe ₃ (SO ₄) ₂ (OH) ₆ ^b	-3230.36	H ₂ AsO ₄ ⁻	-753.399	HS ⁻	12.44438	AgS ⁻	59.968
H ₂ O	-237.177	H ₃ AsO ₃ (a)	-638.142	HS ₂ O ₃ ⁻	-532.363	Ag(SO ₃) ⁻	-441.572
		H ₃ AsO ₄ (a)	-764.001	H ₂ S (a)	-27.656	Ag(SO ₃) ₂ ³⁻	-946.744
		HAsO ₂ (a)	-402.951			Ag(SO ₃) ₃ ⁵⁻	-1434.875
						Ag(S ₂ O ₃) ⁻	-490.262
						Ag(S ₂ O ₃) ₂ ³⁻	-1023.386
						Ag(S ₂ O ₃) ₃ ⁵⁻	-2241.344

^a Data from HSC database 6.0 [23] and Thermochemical Data of Pure Substances [30]. ^b ΔG°_{298} value was calculated using the equation of $\Delta G_r^\circ = -RT \ln K = \sum [v_i \Delta G_f^\circ(i)]$, where $\ln K$ was from the Hydrochemical log K Database of HYDRA/MEDUSA software [31] and relevant ΔG_f° values are listed in Appendix A.

References

- Corkhill, C.L.; Vaughan, D.J. Arsenopyrite oxidation—A review. *Appl. Geochem.* **2009**, *24*, 2342–2361. [CrossRef]
- Márquez, M.A.; Ospina, J.D.; Morales, A.L. New insights about the bacterial oxidation of arsenopyrite: A mineralogical scope. *Miner. Eng.* **2012**, *39*, 248–254. [CrossRef]
- Liu, X.; Xu, B.; Min, X.; Li, Q.; Yang, Y.; Jiang, T.; He, Y.; Zhang, X. Effect of pyrite on thiosulfate leaching of gold and the role of ammonium alcohol polyvinyl phosphate (AAPP). *Metals* **2017**, *7*, 278. [CrossRef]
- Mikhlin, Y.L.; Romanchenko, A.S.; Asanov, I.P. Oxidation of arsenopyrite and deposition of gold on the oxidized surfaces: A scanning probe microscopy, tunneling spectroscopy and XPS study. *Geochim. Cosmochim. Acta* **2006**, *70*, 4874–4888. [CrossRef]
- Fomchenko, N.V.; Muravyov, M. Thermodynamic and XRD analysis of arsenopyrite biooxidation and enhancement of oxidation efficiency of gold-bearing concentrates. *Int. J. Miner. Process.* **2014**, *133*, 112–118. [CrossRef]
- Liu, X.; Li, Q.; Zhang, Y.; Jiang, T.; Yang, Y.; Xu, B.; He, Y. Improving gold recovery from a refractory ore via Na₂SO₄ assisted roasting and alkaline Na₂S leaching. *Hydrometallurgy* **2019**, *185*, 133–141. [CrossRef]
- Liu, X.; Li, Q.; Zhang, Y.; Jiang, T.; Yang, Y.; Xu, B.; He, Y. Simultaneous removal of S and As from a refractory gold ore in a single stage O₂-enriched roasting process. *Metall. Mater. Trans. B* **2019**, *50*, 1588–1596. [CrossRef]
- Miller, P.; Brown, A.R.G. Bacterial Oxidation of Refractory Gold Concentrates. In *Gold Ore Processing: Project Development and Operations*; Adams, M.D., Ed.; Elsevier: Amsterdam, The Netherlands, 2016; pp. 359–372.
- Craw, D.; Falconer, D.; Youngson, J.H. Environmental arsenopyrite stability and dissolution: Theory, experiment, and field observations. *Chem. Geol.* **2003**, *199*, 71–82. [CrossRef]
- Fantauzzi, M.; Licheri, C.; Atzei, D.; Loi, G.; Elsener, B.; Rossi, G.; Rossi, A. Arsenopyrite and pyrite bioleaching: Evidence from XPS, XRD and ICP techniques. *Anal. Bioanal. Chem.* **2011**, *401*, 2237–2248. [CrossRef] [PubMed]
- Henao, D.M.O.; Godoy, M.A.M. Jarosite pseudomorph formation from arsenopyrite oxidation using *Acidithiobacillus ferrooxidans*. *Hydrometallurgy* **2010**, *104*, 162–168. [CrossRef]

12. Pathak, A.; Morrison, L.; Healy, M.G. Catalytic potential of selected metal ions for bioleaching, and potential techno-economic and environmental issues: A critical review. *Bioresour. Technol.* **2017**, *229*, 211–221. [[CrossRef](#)]
13. Zhang, Y.; Li, Q.; Liu, X.; Yin, H.; Yang, Y.; Xu, B.; Jiang, T.; He, Y. The catalytic effect of copper ion in the bioleaching of arsenopyrite by *Acidithiobacillus ferrooxidans* in 9K culture medium. *J. Clean. Prod.* **2020**, *256*, 120391. [[CrossRef](#)]
14. Abdollahi, H.; Shafaei, S.Z.; Noaparast, M.; Manafi, Z.; Niemelä, S.I.; Tuovinen, O.H. Mesophilic and thermophilic bioleaching of copper from a chalcopyrite-containing molybdenite concentrate. *Int. J. Miner. Process.* **2014**, *128*, 25–32. [[CrossRef](#)]
15. Feng, S.; Yang, H.; Xin, Y.; Gao, K.; Yang, J.; Liu, T.; Zhang, L.; Wang, W. A novel and highly efficient system for chalcopyrite bioleaching by mixed strains of *Acidithiobacillus*. *Bioresour. Technol.* **2013**, *129*, 456–462. [[CrossRef](#)]
16. Nazari, G.; Dixon, D.G.; Dreisinger, D.B. The mechanism of chalcopyrite leaching in the presence of silver-enhanced pyrite in the Galvanox™ process. *Hydrometallurgy* **2012**, *113–114*, 122–130. [[CrossRef](#)]
17. Zhao, H.; Wang, J.; Gan, X.; Hu, M.; Zhang, E.; Qin, W.; Qiu, G. Cooperative bioleaching of chalcopyrite and silver-bearing tailing by mixed moderately thermophilic culture: An emphasis on the chalcopyrite dissolution with XPS and electrochemical analysis. *Miner. Eng.* **2015**, *81*, 29–39. [[CrossRef](#)]
18. Guo, P.; Zhang, G.; Cao, J.; Li, Y.; Fang, Z.; Yang, C. Catalytic effect of Ag^+ and Cu^{2+} on leaching realgar (As_2S_2). *Hydrometallurgy* **2011**, *106*, 99–103. [[CrossRef](#)]
19. Zhang, G.; Chao, X.; Guo, P.; Cao, J.; Yang, C. Catalytic effect of Ag^+ on arsenic bioleaching from orpiment (As_2S_3) in batch tests with *Acidithiobacillus ferrooxidans* and *Sulfobacillus sibiricus*. *J. Hazard. Mater.* **2015**, *283*, 117–122. [[CrossRef](#)]
20. Fang, F.; Zhong, H.; Jiang, F.; Zhan, X. Catalytic effect of silver on bioleaching of arsenopyrite. *Int. J. Chem. Eng. Appl.* **2014**, *5*, 474–478. [[CrossRef](#)]
21. Liu, X.; Li, Q.; Zhang, Y.; Yang, Y.; Xu, B.; Jiang, T. Formation process of the passivating products from arsenopyrite bioleaching by *Acidithiobacillus ferrooxidans* in 9K culture medium. *Metals* **2019**, *9*, 1320. [[CrossRef](#)]
22. Liu, X.; Li, Q.; Zhang, Y.; Jiang, T.; Yang, Y.; Xu, B.; He, Y. Electrochemical behaviour of the dissolution and passivation of arsenopyrite in 9K culture medium. *Appl. Surf. Sci.* **2020**, *508*, 145269. [[CrossRef](#)]
23. Roine, A. Outokumpu HSC Chemistry for Windows: Chemical reaction and equilibrium software with extensive thermochemical database. In *User's Guide, Version 6.0*; Outokumpu Research Oy: Pori, Finland, 2006.
24. Lázaro, I.; Cruz, R.; González, I.; Monroy, M. Electrochemical oxidation of arsenopyrite in acidic media. *Int. J. Miner. Process.* **1997**, *50*, 63–75. [[CrossRef](#)]
25. Cruz, R.; Lázaro, I.; Rodríguez, J.M.; Monroy, M.; González, I. Surface characterization of arsenopyrite in acidic medium by triangular scan voltammetry on carbon paste electrodes. *Hydrometallurgy* **1997**, *46*, 303–319. [[CrossRef](#)]
26. Liu, J.Y.; Tao, X.X.; Cai, P. Study of formation of jarosite mediated by *thiobacillus ferrooxidans* in 9K medium. *Procedia Earth Planet. Sci.* **2009**, *1*, 706–712. [[CrossRef](#)]
27. Wang, H.; Bigham, J.M.; Jones, F.S.; Tuovinen, O.H. Synthesis and properties of ammoniojarosites prepared with iron-oxidizing acidophilic microorganisms at 22–65 °C. *Geochim. Cosmochim. Acta* **2007**, *71*, 155–164. [[CrossRef](#)]
28. Qorbani, M.; Gholami, M.; Moradlou, O.; Naseri, N.; Moshfegh, A.Z. Optimal Ag_2S nanoparticle incorporated TiO_2 nanotube array for visible water splitting. *RSC Adv.* **2014**, *4*, 7838–7844.
29. Ristova, M.; Ristov, M. XPS profile analysis on CdS thin film modified with Ag by an ion exchange. *Appl. Surf. Sci.* **2001**, *181*, 68–77. [[CrossRef](#)]
30. Barin, I. *Thermochemical Data of Pure Substances*, 3rd ed.; Wiley-VCH: Weinheim, Germany, 1995.
31. Puigdomenech, I. Make equilibrium diagrams using sophisticated algorithms (MEDUSA). In *Inorganic Chemistry*; Royal Institute of Technology: Stockholm, Sweden, 2004.

